PHYSICAL REVIEW D **82,** 085003 (2010)

Two-dimensional $\mathcal{N} = (2, 2)$ Wess-Zumino model in the functional renormalization group approach

Franziska Synatschke-Czerwonka,[1] Thomas Fischbacher,[2] and Georg Bergner[3]

[1]*Theoretisch-Physikalisches Institut, Friedrich-Schiller-Universität Jena, Max-Wien-Platz 1, D-07743 Jena, Germany*
[2]*University of Southampton, School of Engineering Sciences, Highfield Campus, University Road, SO17 1BJ Southampton, United Kingdom*
[3]*Institut für Theoretische Physik, Westfälische Wilhelms-Universität Münster, Wilhelm-Klemm-Strasse 9, 48149 Münster, Germany*

(Received 22 June 2010; published 1 October 2010)

We study the supersymmetric $\mathcal{N} = (2, 2)$ Wess-Zumino model in two dimensions with the functional renormalization group. At leading order in the supercovariant derivative expansion we recover the nonrenormalization theorem which states that the superpotential has no running couplings. Beyond leading order the renormalization of the bare mass is caused by a momentum-dependent wave function renormalization. To deal with the partial differential equations we have developed a numerical toolbox called FLOWPY. For weak couplings the quantum corrections to the bare mass found in lattice simulations are reproduced with high accuracy. But in the regime with intermediate couplings higher-order operators that are not constrained by the nonrenormalization theorem yield the dominating contribution to the renormalized mass.

DOI: 10.1103/PhysRevD.82.085003 PACS numbers: 05.10.Cc, 12.60.Jv, 02.60.Cb

I. INTRODUCTION

In the search for high energy theories beyond the standard model supersymmetric models are a topic of great interest. Supersymmetry reduces the hierarchy and the fine-tuning problem. It has to be broken at some energy scale since supersymmetry has not been observed in low energy physics. The breaking does not occur on the perturbative level and therefore nonperturbative tools are needed to analyze these models, e.g. lattice formulations or the function renormalization group.

Lattice formulations and simulations have been successfully applied to nonperturbative problems in field theory. Although there has been considerable progress in the last years [1–4] there are still some difficulties in the lattice formulation of supersymmetry. The discretization leads to a (partial) breaking of supersymmetry and the implementation of dynamical fermions on the lattice still poses a challenge.

Nonperturbative continuum methods, such as the functional renormalization group (FRG) which manifestly preserve supersymmetry, can complement the lattice calculations. The FRG has previously been applied to a wide range of nonperturbative problems such as critical phenomena, fermionic systems, gauge theories and quantum gravity; see e.g. [5–13] for reviews. Applied to supersymmetric theories it circumvents problems of the lattice formulation such as supersymmetry breaking due to discretization. But in order to solve the FRG equations truncations have to be employed which introduce a different kind of error.

Quite a few conceptual studies of supersymmetric theories in the framework of the FRG have already been performed. The main ingredient is the construction and use of a manifestly supersymmetric regularization scheme. For example such a regulator has been presented for the four-dimensional Wess-Zumino model in [14,15]. Investigations for one-, two-, and three-dimensional $\mathcal{N} = 1$ Wess-Zumino models have been performed in [16–19]. A FRG formulation of supersymmetric Yang-Mills theory employing the superfield formalism has been given in [20]; for further applications see also [21,22]. General theories of a scalar superfield including the Wess-Zumino model were studied with a Polchinski-type RG equation in [11], which yields a new approach to supersymmetric nonrenormalization theorems. The nonrenormalization theorem has also been proven with FRG methods in [23]. In [24] a Wilsonian effective action for the Wess-Zumino model by perturbatively iterating the FRG is constructed.

The aim of this work is twofold. On the one hand, we want to compare the results from the supersymmetric formulation of the FRG equations to lattice data for the renormalized mass in the two-dimensional $\mathcal{N} = (2, 2)$ Wess-Zumino model [4]. This comparison allows us to estimate the truncation error. The renormalized mass is defined as the location of the pole of the propagator in the complex plane; therefore we have to take the momentum dependence in the FRG framework into account.

There are several applications, where this dependence is important but the related contributions lead to a much higher numerical effort for the solution of the flow equations. Full momentum dependence of propagators and vertices has previously been treated successfully in the literature [25–32]. We introduce a numerical toolbox called FLOWPY which is designed to solve the flow equations with momentum dependence as encountered in this paper. FLOWPY can be adapted to solve not only flow equations with momentum dependence but also other differential equations encountered in the FRG framework e.g. for field

dependent effective potentials. In this paper we demonstrate that FLOWPY solves the flow equations reliably.

The paper is organized as follows: In Sec. II we introduce the $\mathcal{N} = (2, 2)$ Wess-Zumino model in two dimensions. In Sec. III we sketch the derivation of the supersymmetric flow equations for the superpotential and the (momentum-dependent) wave function renormalization. The flow equation for the superpotential will lead to the nonrenormalization theorem. In Sec. IV first FLOWPY is described and then we specialize our flow equations and demonstrate that perturbation theory is reproduced correctly. In Sec. V we compare the renormalized mass calculated in the FRG approach with the results from lattice simulations.

II. THE $\mathcal{N} = (2, 2)$ WESS-ZUMINO MODEL IN TWO DIMENSIONS

The $\mathcal{N} = (2, 2)$ Wess-Zumino model in two dimensions can be found by a dimensional reduction of the $\mathcal{N} = 1$ model in four dimensions [33]. The Lagrange density is given by

$$\mathcal{L} = 2\bar{\partial}\,\bar{\phi}\,\partial\phi + \bar{\psi}M\psi - \tfrac{1}{2}\bar{F}F + \tfrac{1}{2}FW'(\phi) + \tfrac{1}{2}\bar{F}\bar{W}'(\phi) \tag{1}$$

with Dirac fermions ψ and $\bar{\psi}$. The fermion matrix M reads

$$M = \partial\!\!\!/ + W''(\phi)P_+ + \bar{W}''(\phi)P_- \tag{2}$$

with $P_\pm = (\mathbb{1} \pm \gamma_*)/2$, $F = F_1 + iF_2$ and $\phi = \phi_1 + i\phi_2$ as well as $\partial = \frac{1}{2}(\partial_1 - i\partial_2)$ and $z = x_1 + ix_2$. The superpotential is denoted by $W(\phi) = u(\phi_1, \phi_2) + iv(\phi_1, \phi_2)$. We work in the Weyl basis with $\gamma^1 = \sigma_1$, $\gamma^2 = -\sigma_2$ and $\gamma_* = i\gamma^1\gamma^2 = \sigma_3$. The complex spinors can be decomposed as $\psi = (\,\psi_1 \quad \psi_2\,)^T$ and $\bar{\psi} = (\,\bar{\psi}_1 \quad \bar{\psi}_2\,)$. The Lagrange density is invariant under the supersymmetry transformations

$$\begin{aligned}
\delta\phi &= \bar{\psi}_1\varepsilon_1 + \bar{\varepsilon}_1\psi_1, & \delta\bar{\phi} &= \bar{\psi}_2\varepsilon_2 + \bar{\varepsilon}_2\psi_2,\\
\delta\bar{\psi}_1 &= -\tfrac{1}{2}F\bar{\varepsilon}_1 - \partial\phi\bar{\varepsilon}_2, & \delta\bar{\psi}_2 &= -\bar{\partial}\,\bar{\phi}\,\bar{\varepsilon}_1 - \tfrac{1}{2}\bar{F}\bar{\varepsilon}_2,\\
\delta\psi_1 &= -\tfrac{1}{2}F\varepsilon_1 + \bar{\partial}\phi\varepsilon_2, & \delta\psi_2 &= \partial\bar{\phi}\varepsilon_1 - \tfrac{1}{2}\bar{F}\varepsilon_2,\\
\delta F &= 2(\partial\bar{\psi}_1\varepsilon_2 - \bar{\varepsilon}_2\bar{\partial}\psi_1), & \delta\bar{F} &= 2(\partial\bar{\psi}_2\varepsilon_1 - \bar{\varepsilon}_1\bar{\partial}\psi_2).
\end{aligned} \tag{3}$$

The superspace formulation of this model is constructed in Appendix A. A detailed discussion of the underlying supersymmetry algebra and a construction of the superspace can be found e.g. in [34].

Integrating out the auxiliary fields yields the on-shell Lagrangian

$$\mathcal{L}_{\text{on}} = 2\bar{\partial}\,\bar{\phi}\,\partial\phi + \tfrac{1}{2}W'(\phi)\bar{W}'(\phi) + \bar{\psi}M\psi. \tag{4}$$

In this paper we will consider the superpotential

$$W(\phi) = \tfrac{1}{2}m\phi^2 + \tfrac{1}{3}g\phi^3. \tag{5}$$

The system has two bosonic ground states which lead to a nonzero Witten index [35]; therefore supersymmetry is never spontaneously broken in the $\mathcal{N} = (2, 2)$ Wess-Zumino model.

A characteristic feature of the $\mathcal{N} = 1$ Wess-Zumino model in four dimensions survives the dimensional reduction, namely, that bosonic and fermionic loop corrections cancel in such a way that the effective superpotential receives no quantum corrections. This is called the nonrenormalization theorem [36–38]. In the two-dimensional model considered here the cancellations even render the model finite. The model has been studied intensively in the literature; see e.g. [3,4,39–41] for lattice simulations.

III. SUPERSYMMETRIC RG FLOW

Following the lines of our previous works [16–19] we construct a manifestly supersymmetric flow equation in the off-shell formulation. Our approach is based on the FRG formulated in terms of a flow equation for the effective average action Γ_k, i.e. the Wetterich equation [42]

$$\partial_k\Gamma_k = \tfrac{1}{2}\mathrm{STr}\{[\Gamma_k^{(2)} + R_k]^{-1}\partial_k R_k\}. \tag{6}$$

The scale dependent Γ_k interpolates between the microscopic action S for $k \to \Lambda$, with Λ denoting the microscopic UV scale, and the full quantum effective action $\Gamma = \Gamma_{k\to 0}$. As the model considered in this paper is UV finite, the cutoff Λ can be set to infinity. The interpolating scale k denotes an infrared (IR) regulator scale below which all fluctuations with momenta smaller than k are suppressed. For $k \to 0$, all fluctuations are taken into account and we arrive at the full solution of the quantum theory in terms of the effective action Γ. The Wetterich equation defines an RG trajectory in the space of action functionals with the classical action S serving as initial condition.

The second functional derivative of Γ_k in Eq. (6) is defined as

$$(\Gamma_k^{(2)})_{ab} = \frac{\vec{\delta}}{\delta\Psi_a}\Gamma_k\frac{\vec{\delta}}{\delta\Psi_b}, \tag{7}$$

where the indices a, b summarize field components, internal and Lorentz indices, as well as spacetime or momentum coordinates. In the present case, we have $\Psi^T = (\phi, \bar{\phi}, F, \bar{F}, \bar{\psi}, \psi)$ where Ψ is not a superfield, but merely a collection of fields. The momentum-dependent regulator function R_k in Eq. (6) establishes the IR suppression of modes below k. In the general case, three properties of the regulator $R_k(p)$ are essential: (i) $R_k(p)|_{p^2/k^2\to 0} > 0$ which implements the IR regularization, (ii) $R_k(p)|_{k^2/p^2\to 0} = 0$ which guarantees that the regulator vanishes for $k \to 0$, and (iii) $R_k(p)|_{k\to\Lambda\to\infty} \to \infty$ which serves to fix the theory at the classical action in the UV. Different functional forms of R_k correspond to different RG trajectories manifesting the RG scheme dependence but the end point $\Gamma_{k\to 0} \to \Gamma$ remains invariant; see e.g. Refs. [8,43–48]. Supersymmetry

is preserved if the regulator contribution to the cutoff action ΔS_k [cf. Eq. (11)] is supersymmetric.

As an ansatz for the effective action we use an expansion in superspace (see Appendix A for our conventions)[1]

$$\Gamma_k = -2\int d^2x \int dy d\bar{y} Z_k^2(\partial\bar{\partial})\bar{\Phi}\Phi - 2\int d^2x \int dy W_k(\Phi) - 2\int d^2x \int d\bar{y}\bar{W}_k(\bar{\Phi}) \quad (8)$$

$$= \int \frac{d^2p}{4\pi^2}\Big[Z_k^2(p^2)\Big(2p^2\bar{\phi}\phi + \bar{\psi} i\not{p}\psi - \frac{1}{2}\bar{F}F\Big) + \frac{1}{2}FW_k' + \frac{1}{2}\bar{F}\bar{W}_k' + \bar{\psi}(W_k'' P_+ + \bar{W}_k'' P_-)\psi\Big]. \quad (9)$$

In contrast to the usual supercovariant derivative expansion we have included those combinations of the supercovariant derivatives that merely reduce to spacetime derivatives. A momentum dependence in W_k is irrelevant as found in Sec. III B. An arbitrary Kähler potential [$K(\bar{\Phi}, \Phi)$ integrated over the whole superspace] is not taken into account here, since we expect only a small influence for the renormalized mass. Another contribution neglected in this truncation comes from the terms of higher than quadratic order in the auxiliary field and the corresponding supersymmetric partner terms, denoted as auxiliary field potential. In the following we will only work with real and imaginary parts ϕ_1, ϕ_2, F_1, F_2.

For this scale dependent effective action the auxiliary fields obey the equations of motion $F = \bar{W}_k'(\phi)/Z_k^2$ and $\bar{F} = W_k'(\phi)/Z_k^2$. This leads to the on-shell action

$$\Gamma_k^{\text{on}} = \int \frac{d^2p}{4\pi^2}\Big[\frac{1}{2}Z_k^2(p^2)p^2\phi\bar{\phi} + \frac{1}{2}\frac{|W_k'(\phi)|^2}{Z_k^2(p^2)} + i\bar{\psi}\not{p}\psi + \bar{\psi}(W_k'' P_+ \bar{W}_k'' P_-)\psi\Big]. \quad (10)$$

A. Supersymmetric regulator

Supersymmetry is preserved if we shift the mass by a momentum-dependent infrared regulator,[2] $m \to m + Z_k^2 \cdot r_1(k, p^2)$ or multiply the wave function renormalization by a momentum-dependent regulator function, $Z_k^2 \to Z_k^2 \cdot r_2(k, p^2)$. Such regulators are the same as the ones used in the previous models [16–19]. To get a regularized path integral R_k is included in terms of the cutoff action ΔS_k. It reads in a matrix notation

$$\Delta S_k = \frac{1}{2}\int \frac{d^2p}{4\pi^2}\bar{\Psi}Z_k^2 R_k^T \Psi^T \quad (11)$$

with $\Psi = (\,\phi_1 \quad \phi_2 \quad F_1 \quad F_2 \quad \psi(-\boldsymbol{p})^T \quad \bar{\psi}(\boldsymbol{p})\,)$ and

$$R_k = \begin{pmatrix} R_k^B & 0 \\ 0 & R_k^F \end{pmatrix} \quad \text{with} \quad R_k^B = \begin{pmatrix} p^2 r_2 \cdot \mathbb{1} & r_1 \cdot \sigma_3 \\ r_1 \cdot \sigma_3 & -r_2 \cdot \mathbb{1} \end{pmatrix} \quad \text{and} \quad R_k^F = \begin{pmatrix} 0 & i\not{p} \cdot r_2 - r_1 \cdot \mathbb{1} \\ i\not{p} \cdot r_2 + r_1 \cdot \mathbb{1} & 0 \end{pmatrix}. \quad (12)$$

With these regulators at hand we can proceed to calculate the flow equation. Inserting ansatz (9) in the flow equation (6), the propagator can be calculated along the lines described in [49]: The fluctuation matrix $\Gamma_k^{(2)} + R_k$ is decomposed into the propagator $\Gamma_0^{(2)} + R_k$ including the regulator functions and a part $\Delta\Gamma_k$ containing all field dependencies. The flow equation (6) is expanded in the number of fields; see Appendix B for the expansion and the explicit matrices.

B. Flow equation for the superpotential—The nonrenormalization theorem

The quantity at leading order in the supercovariant derivative expansion is the scale dependent superpotential. We obtain the flow equation by projecting onto the terms linear in the auxiliary fields. We can choose either the real or imaginary part of the auxiliary field as they are bound to give the same results due to supersymmetry. The superpotential $W(\phi) = u(\phi_1, \phi_2) + iv(\phi_1, \phi_2)$ is a holomorphic function of ϕ_1 and ϕ_2, and therefore its real and imaginary parts obey the Cauchy-Riemann differential equations

$$\frac{\partial u}{\partial \phi_1} = \frac{\partial v}{\partial \phi_2}, \qquad \frac{\partial u}{\partial \phi_2} = -\frac{\partial v}{\partial \phi_1}. \quad (13)$$

Using these equations we find for the flow equations of the superpotential

$$\partial_k u_k = 0, \qquad \partial_k v_k = 0 \Rightarrow \partial_k W_k = \partial_k \bar{W}_k = 0. \quad (14)$$

This means that the superpotential remains unchanged during the RG flow. The Kähler potential does therefore not influence the flow of the superpotential, as found in [37]. Even the nontrivial momentum dependence considered here does not change this result. The nonrenormalization theorem is verified by the flow equations in the present truncation. This result is similar to the proofs in four dimensions discussed in [11,23].

As the flow vanishes at leading order, the first quantity with a nonvanishing flow is the wave function renormalization which is a term at next-to-leading order in our truncation. It will turn out later that the momentum dependence is important for the renormalized mass (cf. Sec. V); therefore we already include it in ansatz (9).

[1]For the Fourier transformation we use the convention $\partial_j \to ip_j$ with the notations $\boldsymbol{p} = (p_1, p_2)^T$ and $p = |\boldsymbol{p}|$ where there is no risk of misunderstanding.

[2]The regulator function is multiplied with the wave function renormalization to ensure reparametrization invariance of the flow equation.

C. Momentum-dependent flow equation for the wave function renormalization

The flow equation for the wave function renormalization can be obtained from a projection onto the terms quadratic in the auxiliary fields. It is derived in Appendix B and reads

$$\begin{aligned}\partial_k Z_k^2(p) = &-8g^2 \int \frac{d^2q}{4\pi^2} \frac{h(\boldsymbol{p}-\boldsymbol{q})h(\boldsymbol{q})}{v(\boldsymbol{q})^2 v(\boldsymbol{p}-\boldsymbol{q})^2} [\partial_k R_1(\boldsymbol{q}-\boldsymbol{p}) \\ &\times M(\boldsymbol{p}-\boldsymbol{q})v(\boldsymbol{q}) + \partial_k R_1(\boldsymbol{q}) M(\boldsymbol{q}) v(\boldsymbol{p}-\boldsymbol{q})] \\ &+ 4g^2 \int \frac{d^2q}{4\pi^2} \frac{h(\boldsymbol{p}-\boldsymbol{q})\partial_k R_2(\boldsymbol{q}) u(\boldsymbol{q}) v(\boldsymbol{p}-\boldsymbol{q})}{v(\boldsymbol{q})^2 v(\boldsymbol{p}-\boldsymbol{q})^2} \\ &+ 4g^2 \int \frac{d^2q}{4\pi^2} \frac{h(\boldsymbol{q})\partial_k R_2(\boldsymbol{q}-\boldsymbol{p}) v(\boldsymbol{q}) u(\boldsymbol{p}-\boldsymbol{q})}{v(\boldsymbol{q})^2 v(\boldsymbol{p}-\boldsymbol{q})^2}\end{aligned} \tag{15}$$

with the abbreviations (recall that $|\boldsymbol{q}| = q$)

$$\begin{aligned} h(\boldsymbol{q}) &= (r_2(q)+1)Z_k^2(q), \qquad M(\boldsymbol{q}) = m + r_1(q)Z_k^2(q), \\ R_i(\boldsymbol{q}) &= r_i(q)Z_k^2(q), \qquad u(\boldsymbol{q}) = M(\boldsymbol{q})^2 - q^2 h^2(\boldsymbol{q}), \\ v(\boldsymbol{q}) &= M(\boldsymbol{q})^2 + q^2 h^2(\boldsymbol{q}). \end{aligned} \tag{16}$$

Here we are dealing with a UV-finite theory and therefore it is sufficient to use the simple, masslike infrared regulator

$$r_1(k, p^2) = k \quad \text{and} \quad r_2(k, p^2) = 0. \tag{17}$$

After a shift in the integration variables in the second part of the integral (15) the flow equation simplifies to

$$\begin{aligned}\partial_k Z_k^2(p) = &-16g^2 \int \frac{d^2q}{4\pi^2} \frac{kZ_k^2(q) + m}{N(\boldsymbol{q})^2 N(\boldsymbol{p}-\boldsymbol{q})} Z_k^2(q) \\ &\times Z_k^2(|\boldsymbol{p}-\boldsymbol{q}|)\partial_k(kZ_k^2(q)),\end{aligned} \tag{18}$$

where we have introduced the abbreviation

$$N(\boldsymbol{q}) = (q^2 Z_k^4(q) + (kZ_k^2(q) + m)^2). \tag{19}$$

In order to deal with the partial differential equation we have developed a (parallelizable) numerical toolbox called FLOWPY. In the next section we present the main ideas behind our numerical setup to solve the momentum-dependent flow equation. A detailed presentation of FLOWPY is deferred to a future paper [50].

IV. NUMERICAL SETUP

Structurally, the flow equation to be solved numerically is of the form

$$\begin{aligned}\partial_k z(k;p) = \int d^n q I[&k; p; q; z(k; f_1(p,q)); \\ &z(k; f_2(p,q)); \ldots; z(k; f_n(p,q))],\end{aligned} \tag{20}$$

where the external momentum p is treated with a discretized grid. While the integrand I may actually also be a function of $\partial_k z(k;p)$, and hence the integral flow equation be given in implicit form only, numerical results suggest that, at least in the model studied here, $\partial_k z(k;p)$ should be sufficiently small to allow an iterative approach, where the integrand is evaluated first under the assumption $\partial_k z(k;p) = 0$, and the result is then used to reevaluate the integrand with a better approximation to $\partial_k z(k;p)$ until convergence is reached. Apart from this conceptual issue, the technology to deal with an evolution equation of this kind is readily available in an accessible form via the SciPy "Scientific Python" extension [51] to the PYTHON [52] programming language. The details of the numerical strategy are described in Appendix C.

As a test for the numerical approximation and the abilities of FLOWPY, we solve the flow of the perturbative wave function renormalization. It is inferred by setting $Z_k(q)$ to its classical value $Z_k(q) \equiv 1$ on the right-hand side of Eq. (18). The perturbative flow with 60 discretization points is shown in Fig. 1 for different values of k.

It is possible to calculate the perturbative expression for $Z^2_{1\text{-loop}}(p)$ analytically from the perturbative flow equation by performing the k integral using $\lim_{k\to\infty} r_1$, $r_2 \to \infty$ and $\lim_{k\to 0} r_1$, $r_2 \to 0$. This yields

$$\begin{aligned} Z^2_{1\text{-loop}} &= 1 + \frac{g^2}{\pi^2} \int \frac{d^2q}{(m^2+q^2)(m^2+|\boldsymbol{q}-\boldsymbol{p}|^2)} \\ &= 1 + 4g^2 \frac{\operatorname{artanh}(p(4m^2+p^2)^{-1/2})}{\pi p\sqrt{4m^2+p^2}}, \end{aligned} \tag{21}$$

which is shown as a solid line in Fig. 1. This shows that possible errors in the numerical calculation of the wave function renormalization with FLOWPY due to discretization, interpolation and the boundary condition $Z_k(q \to \infty) = 1$ are under control. We will consider Z_k and the renormalized masses obtained from it as exact in the employed truncation.

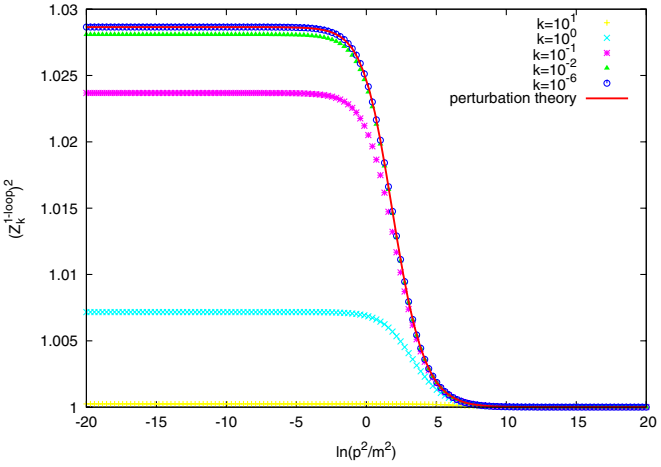

FIG. 1 (color online). Perturbative flow for the parameters $\lambda = g/m = 0.3$ and $m = 1$. The solid line is the plot of Eq. (21).

In the next section we will determine renormalized masses from the nonperturbative wave function renormalization with full momentum dependence calculated with FLOWPY.

V. THE RENORMALIZED MASS

The analytic continuation of the bosonic propagator

$$G_{\text{bos}}(p) = \frac{1}{p^2 + m^2 + \Sigma(p, m, g)} \tag{22}$$

has a pole which defines the renormalized mass. Since the bare mass m is a parameter of the superpotential (5) it is not changed during the flow. Σ is the self-energy. As expected from a supersymmetric theory, the pole of the fermionic propagator leads to the same renormalized mass as the bosonic propagator.

The Fourier transformation of $G_{\text{bos}}(p)$ yields the correlator

$$C_{\text{bos}}(x_1) = \int \frac{dp}{2\pi} G(p_1, 0) e^{ip_1 x_1}. \tag{23}$$

The renormalized mass can be obtained from the long range exponential decay of this quantity and is in the following denoted as *correlator* mass m_{corr}. One can also define a renormalized mass, which we denote as a *propagator* mass, through $m^2_{\text{prop}} = (G_{\text{bos}}(p))^{-1}|_{p=0}$.

To compare the renormalized masses from the FRG with the results of the lattice simulation [4] we consider the masses of the particles in the on-shell theory. In our truncation the bosonic propagator from the on-shell action (10) reads in the infrared limit

$$G^{\text{NLO}}_{\text{bos}}(p) = \frac{1}{p^2 Z^2_{k\to 0}(p^2) + m^2/Z^2_{k\to 0}(p^2)}, \tag{24}$$

and the fermionic propagator reads

$$G^{\text{NLO}}_{\text{ferm}}(p) = \frac{\not{p}}{p^2 Z^4_{k\to 0}(p^2) + m^2}. \tag{25}$$

Both propagators have the same poles and therefore lead to the same renormalized masses for bosons and fermions.

For the propagator mass the fields in the on-shell action have to be rescaled with the wave function renormalization such that the kinetic term is of the canonical form. Neglecting the momentum dependence in the wave function renormalization we obtain

$$m_{\text{prop}} = \frac{m}{Z^2_{k\to 0}(p = 0)}. \tag{26}$$

For a small self-energy Σ a comparison between Eqs. (22) and (24) leads to the approximate relation

$$Z^2_{k\to 0}(p) = 1 + \frac{\Sigma(p, m, g)}{p^2 - m^2}. \tag{27}$$

A numerical calculation can provide $Z^2_k(p)$ only for real p and its analytic continuation cannot be determined straightforwardly. Instead we consider the discrete Fourier transformation of $G^{\text{NLO}}_{\text{bos}}(p)$ with momenta $p = \{0, 2\pi/aN, \ldots, 2\pi(N-1)/aN\}$ on the interval $x \in [0, aN = L]$. For distances much smaller than L this should approximate $C^{\text{NLO}}_{\text{bos}}(x)$ in a well-defined way. More precisely, instead of the exponential decay one gets the long distance behavior

$$C_{a,m_{\text{cor}}}(x_1) \propto \cosh(m_{\text{corr}}(x_1 - L/2)) \tag{28}$$

after the integration over the spatial direction. The mass can be determined from a fit to this function, as it is done in lattice simulations. The details of this procedure can be found in Appendix D.

With the analytic result (21) for $Z^2_{1\text{-loop}}$ at hand we can calculate the poles of $G^{\text{NLO}}_{\text{bos}}(p)$ and obtain a perturbative approximation of m_{corr}. Note that this analytic solution of the perturbative flow together with Eq. (27) leads to the same result as a one-loop *on-shell* calculation of the polarization Σ (cf. Appendix E). Expanding the pole of the propagator (22) to first order in the dimensionless parameter $\lambda^2 = g^2/m^2$ leads to the one-loop approximation of the renormalized mass

$$(m^{1\text{-loop}}_{\text{corr}})^2 = m^2\left(1 - \frac{4}{\sqrt{27}}\lambda^2 + \mathcal{O}(\lambda^4)\right). \tag{29}$$

A. Weak couplings

Let us start with an investigation of the weak coupling sector which is defined as $\lambda < 0.3$, where perturbation theory provides an excellent cross-check to establish the correctness of our ansatz and the errors in the numerical approximation.

The bare mass in the lattice simulations [4] is taken to be $m = 15$. Concerning the units of the mass note the following: In the lattice calculation, the mass is measured in units of the box size, i.e. the physical volume of the lattice simulation. Similarly, everything can be reformulated in terms of the dimensionless ratio of bare and renormalized mass.

For the numerical treatment of Eq. (18) we have to use dimensionless quantities. Because of the nonrenormalization theorem the bare mass quantities in the superpotential enter in the flow equation only as parameters. Rescaling the dimensionful quantities with the bare mass sets the scale in this model. We have set this scale to $m = 1$. To get the same units as in the lattice simulations the resulting renormalized mass is multiplied with 15.

The correlator masses in the weak coupling regime are calculated with the momentum-dependent wave function renormalization from the flow equation (18) solved with FLOWPY. The technical details of the determination of the correlator masses are described in Appendix D. The results are shown in the second column of Table I. The values in the fourth column are taken from a Monte Carlo simulation

TABLE I. Renormalized masses obtained with the flow equation with and without momentum dependence ($m_{\mathrm{corr}}^{\mathrm{FRG}}$ and $m_{\mathrm{prop}}^{\mathrm{FRG}}$) as well as lattice data $m_{\mathrm{corr}}^{\mathrm{lattice}}$ from a continuum extrapolation [4] in the weak coupling regime.

λ	$m_{\mathrm{corr}}^{\mathrm{FRG}}$	$m_{\mathrm{prop}}^{\mathrm{FRG}}$	$m_{\mathrm{corr}}^{\mathrm{lattice}}$
0.02	14.998	14.998	14.999(1)
0.04	14.991	14.992	14.993(3)
0.06	14.979	14.983	14.977(4)
0.08	14.963	14.970	14.963(5)
0.10	14.943	14.952	14.935(6)
0.12	14.917	14.931	14.905(9)
0.14	14.888	14.907	14.871(9)
0.16	14.854	14.878	14.83(1)
0.18	14.815	14.846	14.82(1)
0.20	14.773	14.810	14.75(2)
0.22	14.674	14.771	14.71(2)
0.24	14.674	14.728	14.63(2)
0.26	14.619	14.681	14.60(2)
0.28	14.559	14.631	14.53(2)
0.30	14.496	14.578	14.45(3)

on the lattice [4]. We discuss the lattice results further in Sec. V B. For the time being it suffices to note the agreement of lattice and perturbative results within the statistical errors. Hence perturbation theory already provides a good check for our results.

In Fig. 2 we show the correlator masses from the flow equation, the lattice simulation and the one-loop result (29) for m_{corr}. The masses calculated from the flow equation agree very well with perturbation theory and with the results from lattice simulations. This can be quantified by comparing the correction to the bare mass $\Delta m_{\mathrm{corr}} = m - m_{\mathrm{corr}}$. We find $\Delta m_{\mathrm{corr}}^{\mathrm{FRG}} / \Delta m_{\mathrm{corr}}^{\mathrm{lattice}} \simeq 0.95$. Taking into account the statistical error of the lattice data no significant difference to the FRG results can be found.

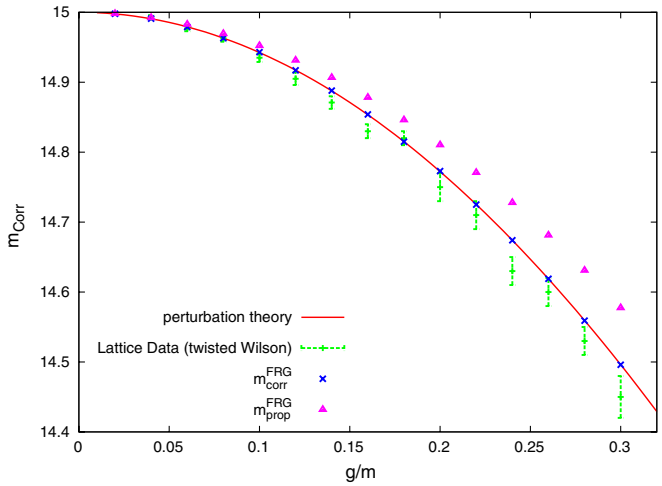

FIG. 2 (color online). Comparison between lattice data taken from [4] and our results for the correlator mass $m_{\mathrm{corr}}^{\mathrm{FRG}}$ *with* momentum dependence and $m_{\mathrm{prop}}^{\mathrm{FRG}}$ without momentum dependence in the weak coupling regime.

We conclude that in the weak coupling regime the truncation of the flow equation with full momentum dependence suffices to capture the main aspects of the model. Higher-order operators, which yield an auxiliary field effective potential, have, as expected, little influence.

To investigate the influence of the momentum dependence in the wave function renormalization, we calculate the propagator mass (26). The results are shown in the third column of Table I and in Fig. 2. A comparison between the propagator mass and the correlator mass from the lattice calculation yields $\Delta m_{\mathrm{prop}}^{\mathrm{FRG}} / \Delta m_{\mathrm{corr}}^{\mathrm{lattice}} \simeq 0.75$. Already in the weak coupling regime it is necessary to include the momentum dependence in order to determine the corrections to the renormalized mass with satisfying accuracy.

B. Intermediate couplings

At intermediate couplings $0.3 \leq \lambda \leq 1$ a significant deviation of our numerical results from perturbation theory can be observed. In this regime the perturbative calculations can no longer provide a reliable test for the numerical results and we have to rely on lattice calculations. In a supersymmetric theory their result must, however, be considered with care as a lattice formulation of supersymmetry still poses difficulties [53]. A common approach is to implement only a part of the supersymmetry which allows one to recover the complete symmetry in the continuum limit in many cases.

In the present model there are further complications for a lattice formulation, especially in the intermediate coupling sector [4]. The considered discretizations are invariant under half of the supersymmetry. They suffer, however, from the dominance of a contribution to the action that is a mere discretization of a surface term at larger couplings. In general the correct continuum limit can only be obtained with unrealistically high numerical effort. The relevance of this effect depends on the coupling strength and on the specific discretization. For intermediate couplings the nonlocal SLAC discretization and the twisted Wilson discretization provides the most reliable results (cf. [4] for details). The renormalized masses of these discretizations are used for a comparison with our results. They are shown in the third and fourth columns of Table II[3] and displayed in Fig. 3 (boxes with error bars) together with the order λ^2 expanded result (29) for m_{corr} (dashed line).

Note that the spontaneous breaking of the $\mathbb{Z}_2$ symmetry introduces also finite volume effects in the lattice simulations. Although there are well-known prescriptions to implement these properties of the theory in lattice simulations, they still lead to additional complications [54].

The correlator masses determined from the FRG are shown in the second column of Table II and displayed in Fig. 3 (crosses). Additionally the perturbative result for the renormalized mass is shown (solid line), which is deter-

[3]All lattice results are extrapolated to the continuum.

TABLE II. Masses obtained with the flow equation with and without momentum dependence ($m_{\mathrm{corr}}^{\mathrm{FRG}}$ and $m_{\mathrm{prop}}^{\mathrm{FRG}}$) as well as lattice data [4] in the regime with intermediate couplings.

λ	$m_{\mathrm{corr}}^{\mathrm{FRG}}$	$m_{\mathrm{prop}}^{\mathrm{FRG}}$	Twisted Wilson	SLAC imp.
0.35	14.321	14.428	14.23(2)	
0.40	14.123	14.259	13.99(3)	14.00(1)
0.45	13.905	14.069	13.62(5)	
0.50	13.666	13.861	13.30(6)	
0.55	13.411	13.636	12.8(1)	
0.60	13.138	13.394	12.2(1)	12.44(6)
0.65	12.854	13.137	11.9(2)	
0.70	12.556	12.866	10.4(5)	
0.75	12.248	12.583		
0.80	11.932	12.290		10.2(3)
0.85	11.609	11.987		
0.90	11.280	11.676		
0.95	10.948	11.358		
1.00	10.613	11.036		8.1(3)[a]

[a]C. Wozar (private communication).

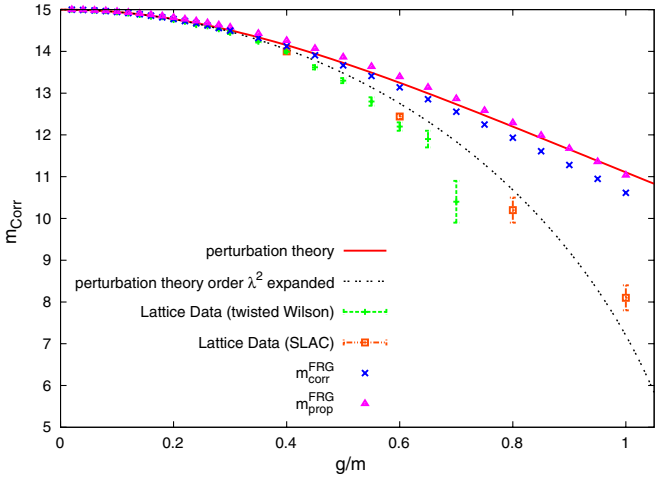

FIG. 3 (color online). Comparison between lattice data taken from [4] and our results for the correlator mass $m_{\mathrm{corr}}^{\mathrm{FRG}}$ *with* momentum dependence and $m_{\mathrm{prop}}^{\mathrm{FRG}}$ without momentum dependence in the intermediate coupling regime.

mined from the pole of the propagator (22) with the polarization calculated in Appendix E.[4]

Although the corrections from the wave function renormalization with full momentum dependence to the bare mass capture some of the quantum effects, they do not account for *all* of the nonperturbative effects present in this model. To quantify this, we compare these corrections to the corrections found in lattice calculations. This yields results between $\Delta m_{\mathrm{corr}}^{\mathrm{FRG}}/\Delta m_{\mathrm{corr}}^{\mathrm{lattice}} \simeq 0.9$ for $\lambda = 0.35$ and $\Delta m_{\mathrm{corr}}^{\mathrm{FRG}}/\Delta m_{\mathrm{corr}}^{\mathrm{lattice}} \simeq 0.65$ for $\lambda = 1.0$. The fact that the wave function renormalization accounts for less of the quantum corrections as the coupling grows is due to the growing influence of higher-order operators, especially the auxiliary field potential. In the present truncation we have only considered terms that are at most quadratic in the auxiliary field and have neglected backreactions from a potential for the auxiliary field. As can be seen from a diagrammatic expansion of the flow equation, terms up to order F_i^4 directly modify the flow equation for the wave function renormalization, which is proportional to F_i^2. It is known from our previous investigations of scalar supersymmetric models [16] that the influence of higher-order operators grows with the strength of the couplings. A truncation that goes beyond the momentum-dependent wave function renormalization has to be considered to improve the results in the regime with intermediate couplings.

The results for the propagator mass are shown in the third column of Table II and in Fig. 3 (triangles). Compared to the lattice results we find $\Delta m_{\mathrm{prop}}^{\mathrm{FRG}}/\Delta m_{\mathrm{corr}}^{\mathrm{lattice}} \simeq 0.75$ for $\lambda = 0.35$ and $\Delta m_{\mathrm{prop}}^{\mathrm{FRG}}/\Delta m_{\mathrm{corr}}^{\mathrm{lattice}} \simeq 0.6$ for $\lambda = 1.0$. The improvement due to the momentum dependence in Z_k^2 is not as pronounced as it is in the weak coupling regime.

VI. CONCLUSIONS

In this paper we have applied the functional renormalization group to the $\mathcal{N} = (2, 2)$ Wess-Zumino model in two dimensions. The model is UV finite which allows a direct comparison to results from lattice simulation.

The first quantity to be calculated in a supercovariant derivative expansion is the superpotential. It is well known from the nonrenormalization theorem that it does not receive quantum corrections. In the language of the FRG the nonrenormalization theorem is recovered in a very simple form, namely, that the superpotential has a vanishing flow equation. The proof only uses the fact that the superpotential is a holomorphic function and therefore the Cauchy-Riemann differential equations for its real and imaginary parts hold.

Hence the first term in the expansion that receives a correction from renormalization is the wave function renormalization. It leads to the renormalization of the bare mass in the on-shell theory, with the renormalized mass defined as the pole of the propagator in the complex plane. We have calculated the renormalized mass with and without momentum dependence in the wave function renormalization.

In order to benchmark our results we use lattice calculations. In the weak coupling regime the results for the

[4]The perturbative results in this regime have to be interpreted with care. The dashed line is an expansion of the on-shell one-loop pole mass to order $\mathcal{O}(\lambda^2)$ whereas the solid line is the result of an off-shell calculation. Both results agree up to order λ^2 but perturbation theory can no longer be trusted in the regime with intermediate coupling strength. The on-shell calculation has to fail at large values of λ^2 because otherwise the renormalized masses will become negative. To preserve supersymmetry in the RG flow the FRG uses an off-shell formulation. Therefore it is not unexpected that it is close to the off-shell perturbation theory.

renormalized mass calculated without the full momentum dependence capture only 75% of the quantum corrections to the bare mass whereas 95% of the corrections are captured if the full momentum dependence in the wave function renormalization is taken into account. This leads to the conclusion that the momentum dependence of wave function renormalization dominates in this regime. Higher-order operators only have a small influence.

For intermediate couplings the picture changes. We have investigated the complete contribution to the flow from the momentum-dependent wave function renormalization. Our findings are that in this truncation only 65% of the quantum corrections to the bare mass determined in the lattice simulations are captured for the largest coupling considered in this paper. Without momentum dependence 60% of the corrections are generated. This leads to the conclusion that in the regime with intermediate couplings the momentum dependence in the wave function renormalization does not include all important contributions to the renormalized mass. Instead, the quantum corrections generated by higher-order-operators which lead to an auxiliary field potential are expected to be relevant for the renormalized mass. They have to be included in order to reduce the deviations between the results from lattice calculations and the FRG. The calculation of these contributions as well as contributions from the Kähler potential remains an interesting challenge for future work.

Although there have been great improvements in the simulations of the model on the lattice they still suffer from finite size effects and the finite lattice spacing, which leads to a breaking of supersymmetry.[5] An interesting application of the FRG is an analysis that includes finite volume effects which could help to estimate the influence of the finite size. This can allow one to separate it from the discretization errors.

The analysis presented in this paper can easily be applied to the $\mathcal{N}=1$ Wess-Zumino model in four dimensions from which the two-dimensional $\mathcal{N}=(2,2)$ model is derived. Especially the nonrenormalization theorem for the superpotential emerges in the same way. In both models the momentum-dependent wave function renormalization is the first relevant contribution in the covariant derivative expansion and the flow equations differ only in the measure of integration. As we have found in the present model the effective potential for the auxiliary field is expected to dominate the quantum effects as the strength of the coupling constant grows.

For the treatment of the partial differential equation we have developed FLOWPY, a numerical toolbox. It can be applied in quite generic situations to solve the FRG equations and to calculate contributions such as the full momentum dependence of vertices. We hope that numerical software like FLOWPY will help to obtain better predictions from FRG calculations. We would like to add that it can also be applied for the calculation of an arbitrary potential $V(\phi)$ instead of the full momentum dependence $Z(p)$. We plan to make FLOWPY available soon [50].

[5]In contrast to common lattice formulations the basic requirements of locality and reflection positivity are broken in the current simulations of this theory. This was done to reduce the unavoidable breaking of supersymmetry on the lattice.

ACKNOWLEDGMENTS

We thank J. Braun, H. Gies, A. Wipf, and C. Wozar for helpful discussions and valuable comments on the manuscript as well as S. Diehl and U. Theis for helpful discussions. F. S. acknowledges support by the Studienstiftung des deutschen Volkes. This work has been supported by the DFG-Research Training Group ''Quantum and Gravitational Fields'' GRK 1523/1.

APPENDIX A: SUPERSPACE FORMULATION

The superspace formulation is constructed from the supersymmetry transformations. The chiral and antichiral superfields can be obtained from the lowest component by acting on it with the exponentiated supersymmetry transformations

$$\begin{aligned}\Phi(z,\bar{z},\alpha,\bar{\alpha}) &= \exp(-\delta_\alpha)\phi(z,\bar{z}) = \sum_{n=0}^{4}\frac{1}{n!}(-\delta_\alpha)^n\phi(z,\bar{z})\\ &= \phi(u,\bar{u}) - \bar{\psi}_1(u,\bar{u})\alpha_1 - \bar{\alpha}_1\psi_1(u,\bar{u})\\ &\quad - \frac{F(u,\bar{u})}{2}\bar{\alpha}_1\alpha_1,\\ \bar{\Phi}(z,\bar{z},\alpha,\bar{\alpha}) &= \exp(-\delta_\alpha)\bar{\phi}(z,\bar{z}) = \sum_{n=0}^{4}\frac{1}{n!}(-\delta_\alpha)^n\bar{\phi}(z,\bar{z})\\ &= \bar{\phi}(u,\bar{u}) - \bar{\psi}_2(u,\bar{u})\alpha_2 - \bar{\alpha}_2\psi_2(u,\bar{u})\\ &\quad - \frac{\bar{F}(u,\bar{u})}{2}\bar{\alpha}_2\alpha_2\end{aligned} \tag{A1}$$

with the chiral variables $u = z - \frac{1}{2}\bar{\alpha}_2\alpha_1$ and $\bar{u} = \bar{z} + \frac{1}{2}\bar{\alpha}_1\alpha_2$. The supercharges are

$$\begin{aligned} Q_1 &= -\frac{\partial}{\partial\bar{\alpha}_1} + \frac{1}{2}\alpha_2\bar{\partial}, & \bar{Q}_1 &= \frac{\partial}{\partial\alpha_1} - \frac{1}{2}\bar{\alpha}_2\partial,\\ Q_2 &= -\frac{\partial}{\partial\bar{\alpha}_2} + \frac{1}{2}\alpha_1\partial, & \bar{Q}_2 &= \frac{\partial}{\partial\alpha_2} - \frac{1}{2}\bar{\alpha}_1\bar{\partial}, \end{aligned} \tag{A2}$$

and the supercovariant derivatives read

$$\begin{aligned} D_1 &= -\frac{\partial}{\partial\bar{\alpha}_1} - \frac{1}{2}\alpha_2\bar{\partial}, & \bar{D}_1 &= \frac{\partial}{\partial\alpha_1} + \frac{1}{2}\bar{\alpha}_2\partial,\\ D_2 &= -\frac{\partial}{\partial\bar{\alpha}_2} - \frac{1}{2}\alpha_1\partial, & \bar{D}_2 &= \frac{\partial}{\partial\alpha_2} + \frac{1}{2}\bar{\alpha}_1\bar{\partial}. \end{aligned} \tag{A3}$$

The superfield obeys the (anti)chiral constraint

$$D_2\Phi = \bar{D}_2\Phi = 0, \qquad D_1\bar{\Phi} = \bar{D}_1\bar{\Phi} = 0. \tag{A4}$$

The supersymmetry transformations are generated by

$$\delta\Phi = (\bar{\varepsilon}Q + \bar{Q}\varepsilon)\Phi, \qquad \delta\bar{\Phi} = (\bar{\varepsilon}Q + \bar{Q}\varepsilon)\bar{\Phi}. \quad \text{(A5)}$$

The Lagrange density is given by

$$\begin{aligned}\mathcal{L} &= \mathcal{L}_{\text{kin}} + \mathcal{L}_{\text{pot}} \\ &= -2\int dy d\bar{y}\,\bar{\Phi}\,\Phi - 2\int dy W(\Phi) - 2\int d\bar{y}\,\bar{W}(\bar{\Phi})\end{aligned} \quad \text{(A6)}$$

with $dy \equiv d\bar{\alpha}_1 d\alpha_1$ and $d\bar{y} \equiv d\alpha_2 d\bar{\alpha}_2$.

APPENDIX B: FLOW EQUATION FOR THE MOMENTUM-DEPENDENT WAVE FUNCTION RENORMALIZATION

To obtain the flow equations for the wave function renormalization we decompose the second derivative of the effective action into a field independent part $\Gamma_0^{(2)} + R_k$ and a field dependent part $\Delta\Gamma_k^{(2)}$ (in the following we drop the momentum dependence of the regulators for simplicity of notation):

$$\begin{aligned}&(\Gamma_0^{(2)} + R_k)(\boldsymbol{q}, \boldsymbol{q}') + \Delta\Gamma_k(\boldsymbol{q}, \boldsymbol{q}') \\ &\quad = \begin{pmatrix} A_0 & 0 \\ 0 & B_0 \end{pmatrix}\delta(\boldsymbol{q} - \boldsymbol{q}') + \begin{pmatrix} \Delta A & 0 \\ \Delta D & \Delta B \end{pmatrix}\end{aligned} \quad \text{(B1)}$$

with $[h = (1 + r_2)Z_k^2(q),\ M = (r_1 Z_k^2(q) + m)]$

$$A_0 = \begin{pmatrix} q^2 h \cdot \mathbb{1} & M \cdot \sigma_3 \\ M \cdot \sigma_3 & -h \cdot \mathbb{1} \end{pmatrix}, \qquad B_0 = i\not{q} h + M\mathbb{1} \quad \text{(B2)}$$

and

$$\begin{aligned}\Delta A &= 2g\begin{pmatrix} F_1 & -F_2 & \phi_1 & -\phi_2 \\ -F_2 & -F_1 & -\phi_2 & -\phi_1 \\ \phi_1 & -\phi_2 & 0 & 0 \\ -\phi_2 & -\phi_1 & 0 & 0 \end{pmatrix}(\boldsymbol{q} + \boldsymbol{q}'), \\ \Delta C &= 2g\begin{pmatrix} \bar{\psi}_1 & i\bar{\psi}_2 \\ \bar{\psi}_1 & -i\bar{\psi}_2 \\ 0 & 0 \\ 0 & 0 \end{pmatrix}(\boldsymbol{q} + \boldsymbol{q}'), \\ \Delta D &= 2g\begin{pmatrix} \psi_1 & i\psi_1 & 0 & 0 \\ \psi_2 & -i\psi_2 & 0 & 0 \end{pmatrix}(\boldsymbol{q} + \boldsymbol{q}'), \\ \Delta B &= 2g\begin{pmatrix} \phi_1 + i\phi_2 & 0 \\ 0 & \phi_1 - i\phi_2 \end{pmatrix}(\boldsymbol{q} + \boldsymbol{q}').\end{aligned} \quad \text{(B3)}$$

The flow equation can then be expanded [49] in

$$\begin{aligned}\partial_t\Gamma_k &= \tfrac{1}{2}\tilde{\partial}_t\,\text{STr}((\Gamma_0^{(2)} + R_k)^{-1}\Delta\Gamma) \\ &\quad - \tfrac{1}{4}\tilde{\partial}_t\,\text{STr}((\Gamma_0^{(2)} + R_k)^{-1}\Delta\Gamma)^2 + \cdots\end{aligned} \quad \text{(B4)}$$

with $\tilde{\partial}_t$ acting only on the regulator. STr denotes a trace in field space as well as an integration in momentum space. The wave function renormalization is a term proportional to F_i^2 and can be obtained from the second term in this expansion. To calculate this we define

$$\begin{aligned}M(\boldsymbol{q}, \boldsymbol{q}') &\equiv \int_{\boldsymbol{q}''}(\Gamma_0^{(2)} + R_k)^{-1}(\boldsymbol{q})\delta(\boldsymbol{q} + \boldsymbol{q}'')\Delta\Gamma(\boldsymbol{q}'', \boldsymbol{q}') \\ &= (\Gamma_0^{(2)} + R_k)^{-1}(\boldsymbol{q})\Delta\Gamma(-\boldsymbol{q}, \boldsymbol{q}')\end{aligned} \quad \text{(B5)}$$

and the second term in the expansion reads

$$\begin{aligned}&\tilde{\partial}_t\,\text{Str}\int_{\boldsymbol{q},\boldsymbol{q}'} M(\boldsymbol{q}, \boldsymbol{q}')M(\boldsymbol{q}', \boldsymbol{q}) \\ &\quad = \text{Str}\int_{\boldsymbol{q},\boldsymbol{q}'}(\Gamma_0^{(2)} + R_k)^{-1}(\boldsymbol{q})\partial_t R_k(\Gamma_0^{(2)} + R_k)^{-1} \\ &\quad \times (\boldsymbol{q})\Delta\Gamma(-\boldsymbol{q}, \boldsymbol{q}')(\Gamma_0^{(2)} + R_k)^{-1}(\boldsymbol{q}')\Delta\Gamma(-\boldsymbol{q}', \boldsymbol{q}) \\ &\quad + \text{Str}\int_{\boldsymbol{q},\boldsymbol{q}'}(\Gamma_0^{(2)} + R_k)^{-1}(\boldsymbol{q})\Delta\Gamma(-\boldsymbol{q}, \boldsymbol{q}')(\Gamma_0^{(2)} + R_k)^{-1} \\ &\quad \times (\boldsymbol{q}')\partial_t R_k(\boldsymbol{q}')(\Gamma_0^{(2)} + R_k)^{-1}(\boldsymbol{q}')\Delta\Gamma(-\boldsymbol{q}', \boldsymbol{q}),\end{aligned} \quad \text{(B6)}$$

where Str denotes a trace in field space. We take the functional derivative with respect to $F_i(\boldsymbol{p})$ and $F_i(-\boldsymbol{p})$ and set all fields to zero in order to project on the wave function renormalization $Z_k(p^2)$. This yields

$$\begin{aligned}\partial_k Z_k^2(p) &= -8g^2\int\frac{d^2q}{4\pi^2}\frac{h(\boldsymbol{p} - \boldsymbol{q})h(\boldsymbol{q})}{v(\boldsymbol{q})^2 v(\boldsymbol{p} - \boldsymbol{q})^2}[\partial_k R_1(\boldsymbol{q} - \boldsymbol{p}) \\ &\quad \times M(\boldsymbol{p} - \boldsymbol{q})v(\boldsymbol{q}) + \partial_k R_1(\boldsymbol{q})M(\boldsymbol{q})v(\boldsymbol{p} - \boldsymbol{q})] \\ &\quad + 4g^2\int\frac{d^2q}{4\pi^2}\frac{h(\boldsymbol{p} - \boldsymbol{q})\partial_k R_2(\boldsymbol{q})u(\boldsymbol{q})v(\boldsymbol{p} - \boldsymbol{q})}{v(\boldsymbol{q})^2 v(\boldsymbol{p} - \boldsymbol{q})^2} \\ &\quad + 4g^2\int\frac{d^2q}{4\pi^2}\frac{h(\boldsymbol{q})\partial_k R_2(\boldsymbol{q} - \boldsymbol{p})v(\boldsymbol{q})u(\boldsymbol{p} - \boldsymbol{q})}{v(\boldsymbol{q})^2 v(\boldsymbol{p} - \boldsymbol{q})^2}\end{aligned} \quad \text{(B7)}$$

with the abbreviations

$$\begin{aligned}h(\boldsymbol{q}) &= (r_2(q) + 1)Z_k^2(q), \qquad M(\boldsymbol{q}) = m + r_1(q)Z_k^2(q), \\ R_i(\boldsymbol{q}) &= r_i(q)Z_k^2(q), \qquad u(\boldsymbol{q}) = M(\boldsymbol{q})^2 - q^2 h^2(\boldsymbol{q}), \\ &\qquad v(\boldsymbol{q}) = M(\boldsymbol{q})^2 + q^2 h^2(\boldsymbol{q}).\end{aligned} \quad \text{(B8)}$$

APPENDIX C: THE COMPUTATIONAL STRATEGY

To solve flow equations depending on an external momentum the computational strategy is as follows:

(i) Mapping the $k \to 0$ flow to a forward time evolution problem by introducing $\tilde{k} = -k$.

(ii) Discretization of the problem by approximating $z(k; p)$ with an interpolation function that is determined by N support points. These are best chosen to be equidistant on a logarithmic scale, accounting for the expectation that a wide range of scales should contribute in a comparable way to the integral.

(iii) For now, we have been using interpolation in conjunction with the two-dimensional integration

function SCIPY.INTEGRATE.DBLQUAD() from Scientific Python. However, this *ad hoc* approach should allow great efficiency improvements by instead considering a tighter integration of numerical quadrature with adaptive discretization. In particular, it should then also be possible to also pass on information about the discretized flow equation's Jacobian matrix to the numerical ordinary differential equation (ODE) integrator. There hence is considerable potential for further efficiency improvements of numerical RG flow code.

(iv) Solving the resulting ordinary differential equation for the values of $z(k;p)$ at the support points with SciPy's SCIPY.INTEGRATE.ODEINT() function (which internally uses LSODA from ODEPACK).

Concerning the numerical solution of the ODE, some manual tweaking of integration parameters such as maximal step sizes is required when the coupling constant g is large and $k \sim m$. We note that, by the very nature of this problem, the computation is readily parallelized: The effort to numerically determine the right-hand side integral is expected to roughly grow like $\mathcal{O}(N^2)$ with the number N of support points, and computations for different support points are independent. In comparison to the computational effort required to compute the integrals, the communication overhead to distribute the values of $z(k;p)$ at different support points is fairly negligible; hence using one of the readily available message passing interface extensions to PYTHON to intelligently distribute the workload becomes an attractive option. One should, however, take care that the core structure of the integrand then is implemented in a compiled (C code) PYTHON extension before even thinking about parallelization.

APPENDIX D: DETERMINATION OF THE RENORMALIZED MASS

The numerical calculations of Z_k^2 in the main text use a grid of $N = 60$ points in the direction of p^2, distributed equidistantly on a logarithmic scale. The result for $Z_{k\to 0}(p)$ is interpolated with splines to calculate the propagator $G_{\mathrm{bos}}^{\mathrm{NLO}}(p)$. A discreet Fourier transformation of $G_{\mathrm{bos}}^{\mathrm{NLO}}(p)$

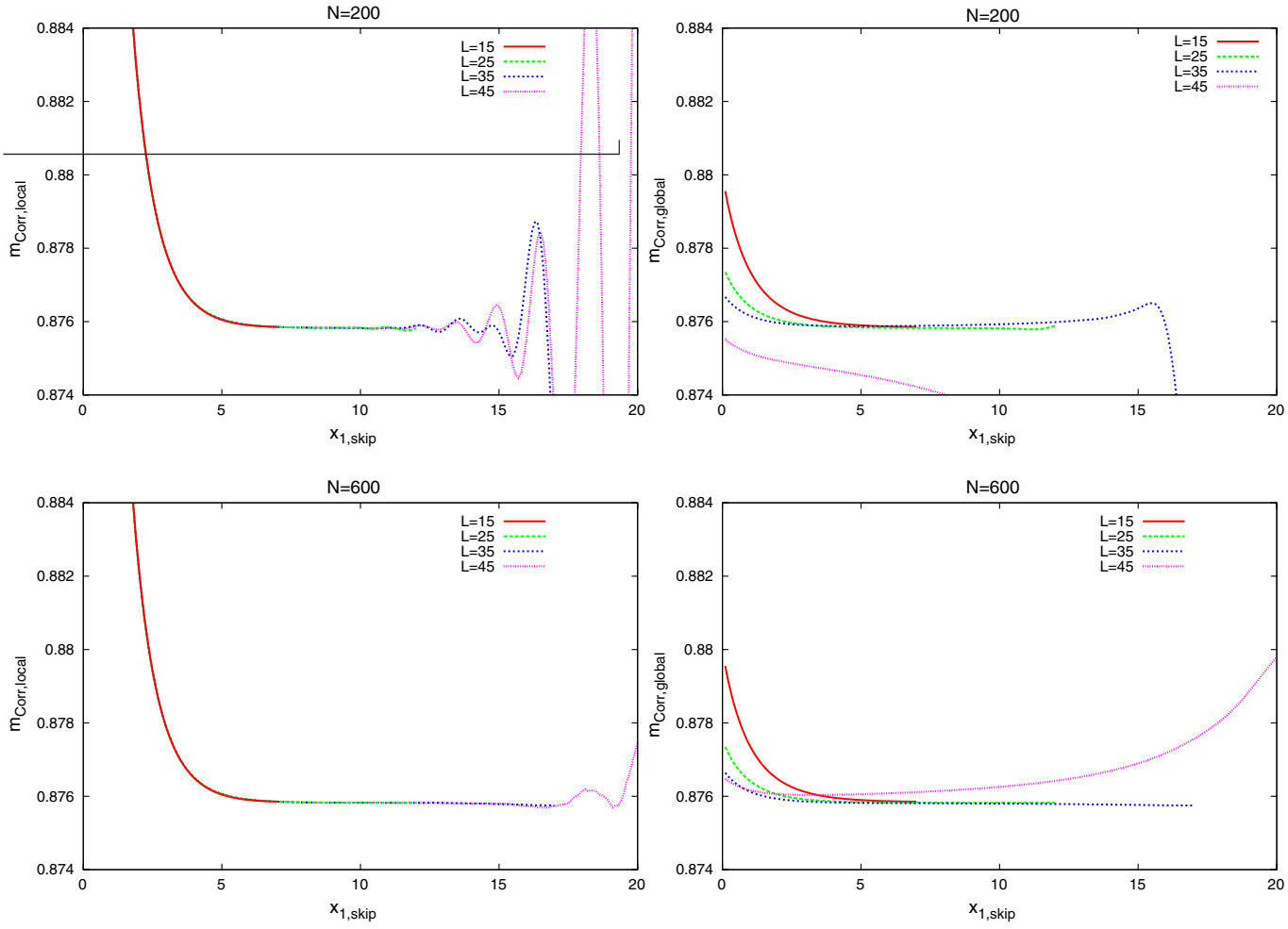

FIG. 4 (color online). Left panel: $m_{\mathrm{corr}}^{\mathrm{local}}$ with $\lambda = 0.6$ for discretizations $N = 200$ and $N = 600$ and different box sizes $L = 15$, 25, 35 and 45. Right panel: $m_{\mathrm{corr}}^{\mathrm{global}}$ with $\lambda = 0.6$ for discretizations $N = 200$ and $N = 600$ and different box sizes $L = 15$, 25, 35 and 45.

yields the correlator $C(x_1)$ on the interval $x_1 \in [0, L]$ with $n = 100\,01$ intermediate points. In the main text we have used $L = 15$. From its large distance behavior

$$C_{a,m_{\rm cor}}(x_1) \propto \cosh(m_{\rm corr}(x_1 - L/2)) \tag{D1}$$

the correlator mass $m_{\rm corr}$ is determined by a least square fit. The fit range is constrained to the interval $[x_{1,\rm skip}, \ldots, L - x_{1,\rm skip}]$ where the contributions of excited states are negligible. The value of $x_{1,\rm skip}$ is determined such that $m_{\rm corr}(x_{1,\rm skip})$ shows a plateau. We can either fit on the whole range $[x_{1,\rm skip}, \ldots, L - x_{1,\rm skip}]$—this quantity is called $m_{\rm corr}^{\rm global}$—or make the fit just inside a small interval of size 0.2 starting from $x_{1,\rm skip}$—this quantity is called $m_{\rm corr}^{\rm local}$.

In the left panel of Fig. 4 $m_{\rm corr}^{\rm local}$ is shown for two different discretizations of $Z_k^2(p^2)$, $N = 200$ in the upper and $N = 600$ in the lower panel. In the right panel the same is shown for $m_{\rm corr}^{\rm global}$. From these plots we can read off that for $x_{1,\rm skip}$ not too large there is a clear plateau which is stable if the box size is increased. But for very large $x_{1,\rm skip}$ the local mass oscillates. As this oscillation is reduced if the discretization is increased it is due to fluctuations in the spline interpolation of Z_k^2. At small values of the correlator the numerical errors are more important for the masses. As the fluctuations become visible for large box sizes, in these cases the global mass fit is of no use because it averages over the local mass and is strongly influenced by the oscillations. We will therefore take the plateau of $m_{\rm corr}^{\rm local}$ as the value of the renormalized mass.

APPENDIX E: PERTURBATION THEORY

In perturbation theory the mass is determined from the one particle irreducible (proper) vertex $\Sigma(p)$. The perturbative expansion of this vertex is

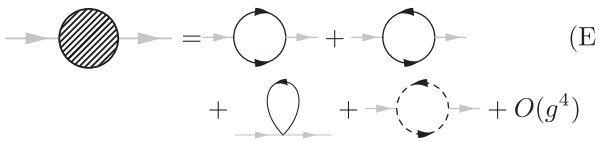

(E1)

$$\begin{aligned}
\Sigma(p) &= 2g^2 \int \frac{d^2s}{4\pi^2} \frac{6m^2 - 4((\boldsymbol{p} - \boldsymbol{s})^2 + m^2)}{(s^2 + m^2)((\boldsymbol{s} - \boldsymbol{p})^2 + m^2)} \\
&\quad + 2g^2 \int \frac{d^2s}{4\pi^2} \frac{4(\boldsymbol{s}^2 - \boldsymbol{s} \cdot \boldsymbol{p} - i\epsilon^{\mu\nu} s_\mu (s_\nu - p_\nu))}{(s^2 + m^2)((\boldsymbol{s} - \boldsymbol{p})^2 + m^2)} \\
&= 2g^2 \int \frac{d^2s}{4\pi^2} \frac{2(m^2 - \boldsymbol{p}^2)}{(s^2 + m^2)((\boldsymbol{s} - \boldsymbol{p})^2 + m^2)} \\
&= 2g^2 \int_0^1 dz \int \frac{d^2s}{4\pi^2} \frac{2(m^2 - p^2)}{(s^2 + z(1 - z)p^2 + m^2)^2} \\
&= 2g^2 \int_0^1 dz \frac{2(m^2 - p^2)}{4\pi(z(1 - z)p^2 + m^2)^2} \\
&= \frac{4g^2(m^2 - p^2)}{\pi p \sqrt{4m^2 + p^2}} \operatorname{artanh}(p(4m^2 + p^2)^{-1/2}).
\end{aligned} \tag{E2}$$

[1] Simon Catterall, David B. Kaplan, and Mithat Unsal, Phys. Rep. **484**, 71 (2009).
[2] Joel Giedt, Int. J. Mod. Phys. A **21**, 3039 (2006).
[3] Georg Bergner, Tobias Kaestner, Sebastian Uhlmann, and Andreas Wipf, Ann. Phys. (N.Y.) **323**, 946 (2008).
[4] Tobias Kastner, Georg Bergner, Sebastian Uhlmann, Andreas Wipf, and Christian Wozar, Phys. Rev. D **78**, 095001 (2008).
[5] K. Aoki, Int. J. Mod. Phys. B **14**, 1249 (2000).
[6] Jurgen Berges, Nikolaos Tetradis, and Christof Wetterich, Phys. Rep. **363**, 223 (2002).
[7] Daniel F. Litim and Jan M. Pawlowski, arXiv:hep-th/9901063.
[8] Jan M. Pawlowski, Ann. Phys. (N.Y.) **322**, 2831 (2007).
[9] Holger Gies, arXiv:hep-ph/0611146.
[10] Hidenori Sonoda, arXiv:0710.1662.
[11] Oliver J. Rosten, J. High Energy Phys. 03 (2010) 004.
[12] O. J. Rosten, arXiv:1003.1366.
[13] B. Delamotte, D. Mouhanna, and M. Tissier, Phys. Rev. B **69**, 134413 (2004).
[14] F. Vian, arXiv:hep-th/9811055.
[15] M. Bonini and F. Vian, Nucl. Phys. **B532**, 473 (1998).
[16] Franziska Synatschke, Georg Bergner, Holger Gies, and Andreas Wipf, J. High Energy Phys. 03 (2009) 028.
[17] Holger Gies, Franziska Synatschke, and Andreas Wipf, Phys. Rev. D **80**, 101701(R) (2009).
[18] Franziska Synatschke, Holger Gies, and Andreas Wipf, Phys. Rev. D **80**, 085007 (2009).
[19] Franziska Synatschke, Jens Braun, and Andreas Wipf, Phys. Rev. D **81**, 125001 (2010).
[20] Sven Falkenberg and Bodo Geyer, Phys. Rev. D **58**, 085004 (1998).
[21] S. Arnone and K. Yoshida, Int. J. Mod. Phys. B **18**, 469 (2004).
[22] Stefano Arnone, Francesco Guerrieri, and Kensuke Yoshida, J. High Energy Phys. 05 (2004) 031.
[23] Hidenori Sonoda and Kayhan Ulker, Prog. Theor. Phys. **123**, 989 (2010).
[24] Hidenori Sonoda and Kayhan Ulker, Prog. Theor. Phys. **120**, 197 (2008).
[25] Ulrich Ellwanger, Manfred Hirsch, and Axel Weber, Z. Phys. C **69**, 687 (1996).
[26] Jan M. Pawlowski, Daniel F. Litim, Sergei Nedelko, and Lorenz von Smekal, Phys. Rev. Lett. **93**, 152002 (2004).

[27] Christian S. Fischer and Holger Gies, J. High Energy Phys. 10 (2004) 048.
[28] Jean-Paul Blaizot, Ramon Mendez-Galain, and Nicolas Wschebor, Phys. Rev. E **74**, 051117 (2006).
[29] Jean-Paul Blaizot, Ramon Mendez-Galain, and Nicolas Wschebor, Phys. Rev. E **74**, 051116 (2006).
[30] Jean-Paul Blaizot, Ramon Mendez-Galain, and Nicolas Wschebor, Phys. Lett. B **632**, 571 (2006).
[31] F. Benitez *et al.*, Phys. Rev. E **80**, 030103 (2009).
[32] S. Diehl, H. C. Krahl, and M. Scherer, Phys. Rev. C **78**, 034001 (2008).
[33] J. Wess and B. Zumino, Phys. Lett. **49B**, 52 (1974).
[34] P. West, *Introduction to Supersymmetry and Supergravity* (World Scientific, Singapore, 1990), extended 2nd ed.
[35] Edward Witten, Nucl. Phys. **B202**, 253 (1982).
[36] Edward Witten, Nucl. Phys. **B403**, 159 (1993).
[37] Kentaro Hori, Sheldon Katz, Albrecht Klemm, Rahul Pandharipande, Richard Thomas, Cumrun Vafa, Ravi Vakil, and Eric Zaslow, *Mirror Symmetry* (Clay Mathematics Institute, Cambridge, MA, 2003).
[38] S. J. Gates, Marcus T. Grisaru, M. Rocek, and W. Siegel, Front. Phys. **58**, 1 (1983).
[39] Matteo Beccaria, Giuseppe Curci, and Erika D'Ambrosio, Phys. Rev. D **58**, 065009 (1998).
[40] Simon Catterall and Sergey Karamov, Phys. Rev. D **68**, 014503 (2003).
[41] Joel Giedt, Nucl. Phys. **B726**, 210 (2005).
[42] Christof Wetterich, Phys. Lett. B **301**, 90 (1993).
[43] Daniel F. Litim, Phys. Lett. B **486**, 92 (2000).
[44] Daniel F. Litim, Phys. Rev. D **64**, 105007 (2001).
[45] Daniel F. Litim and Jan M. Pawlowski, Phys. Lett. B **516**, 197 (2001).
[46] Daniel F. Litim, Nucl. Phys. **B631**, 128 (2002).
[47] Daniel F. Litim and Jan M. Pawlowski, J. High Energy Phys. 11 (2006) 026.
[48] L. Canet, B. Delamotte, D. Mouhanna, and J. Vidal, Phys. Rev. D **67**, 065004 (2003).
[49] Holger Gies and Christof Wetterich, Phys. Rev. D **65**, 065001 (2002).
[50] Thomas Fischbacher and Franziska Synatschke (work in progress).
[51] http://www.scipy.org/.
[52] http://lucas.iquanta.info/linux/Python/docs/docs/official_2_5/ref.pdf.
[53] Georg Bergner, J. High Energy Phys. 01 (2010) 024.
[54] G. Bergner and C Wozar (unpublished).